Progress In Electromagnetics Research Letters, Vol. 61, 63–69, 2016

A Design of Quasi-Arbitrary Phase Difference Unequal Microstrip Power Divider

Qing He[1], Xiaochen Meng[1], Xiaoping Lou[2], and Lianqing Zhu[3, *]

Abstract—An unequal power divider which features quasi-arbitrary output phase difference is proposed in this paper. The circuit consists of four microstrip lines and a resister. By the even- and odd-mode analysis technique, the closed-form design equations of this structure are derived. The characteristic impedances, electrical length and bandwidth variations with power division ratio and phase difference are analyzed. For proving its validity, a prototype with this proposed structure is designed and implemented at 1 GHz. The results of simulation and measurement show that the proposed power divider can effectively produce two outputs with controllable power division and phase difference.

1. INTRODUCTION

Power divider is one of the essential building blocks used in microwave and millimeter-wave systems to provide arbitrary power division outputs with constant phase difference [1–3]. Its characteristic allows it to be widely applied in feeding networks of antennas and high-efficient power amplifiers [4, 5]. With the development of radio frequency (RF) technology, the actual requirement for feeding networks is not only unequal power division, but also arbitrary phase difference [6]. Recently, extensive researches about power dividers have been focused on size reduction, high power division and dual-band applications [7–9]. However, the output arbitrary phase difference characteristic was rarely discussed, which limits its use.

In previous research work, a three-port power divider and phase shifters are connected to realize the function of an unequal power divider and arbitrary phase difference, such as in Butler matrixes, amplifier and mixer [6, 10, 11]. The main disadvantages of these phase shifters are the intolerable bandwidth reduction and insertion loss. On the other hand, they are undesirable for miniaturization and low-cost system. Although there are some power divider designs for 45, 90 or 180 degree phase difference [12–15], they cannot satisfy the requirement of arbitrary phase difference for flexible applications.

In this paper, we present a quasi-arbitrary phase difference power divider. This structure is composed of four microstrip lines and a matching resister which can be fabricated easily on a printed circuit board (PCB) with a low cost. Under the given power division and phase difference, the circuit parameters can be calculated by explicit design formulas. In addition, the characteristic impedances, electrical lengths and bandwidths variations with power division ratio and phase difference are analyzed. An experimental prototype has been designed, fabricated and measured. The measured results agree with the simulated ones closely. The simulated and measured results demonstrate reasonable performance of quasi-arbitrary phase difference, unequal power division, impedance matching and isolation among the output ports.

Received 25 March 2016, Accepted 15 June 2016, Scheduled 13 July 2016

* Corresponding author: Lianqing Zhu (42033768@qq.com).

[1] Beijing Key Laboratory for Optoelectronics Measurement Technology, China. [2] Beijing Engineering Research Center of Optoelectronic Information and Instruments, China. [3] Beijing Laboratory for Biomedical Detection Technology and Instrument, Beijing Information Science and Technology University, Beijing, China.

2. THEORY AND DESIGN EQUATIONS

Figure 1 shows a topology diagram of the proposed quasi-arbitrary phase difference power divider. The four transmission lines are connected as a circle while three ports and the matching resister are located in the joint points, respectively. Port 1 is input port, and ports 2 and 3 are output ports. The corresponding characteristic impedances Z_i and electrical lengths θ_i at the operating frequency of these transmission lines are labeled in Figure 1 ($i = a, b, c$). To simplify the theoretical analysis, the structure is designed as an axis symmetry form. Therefore, the matching resister equals the port impedance Z_0, and the circuit can be divided into even- and odd-mode equivalent subcircuits as shown in Figure 2.

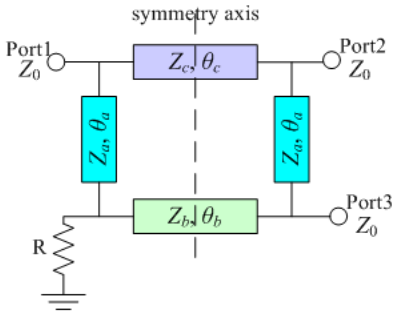

Figure 1. Topology diagram of the power divider with quasi-arbitrary power division ratio and phase difference.

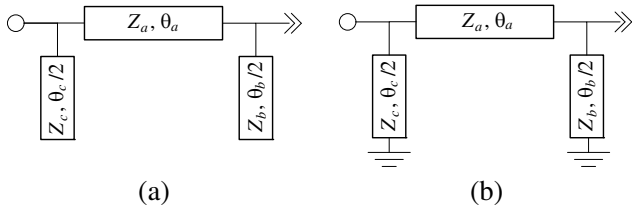

Figure 2. (a) Even- and (b) odd-mode equivalent subcircuits of power divider.

Under the assumption that the transmission lines are lossless, $ABCD$ parameters of the even- and odd-mode equivalent circuits are obtained as:

$$\begin{bmatrix} A_e & B_e \\ C_e & D_e \end{bmatrix} = \begin{bmatrix} \cos\theta_a - \frac{Z_a \sin\theta_a \tan\frac{\theta_b}{2}}{Z_b} & \mathrm{j}Z_a \sin\theta_a \\ \mathrm{j}\left(\frac{\tan\frac{\theta_c}{2}\cos\theta_a}{Z_c} + \frac{\sin\theta_a}{Z_a} - \frac{Z_a \sin\theta_a \tan\frac{\theta_c}{2}\tan\frac{\theta_b}{2}}{Z_c Z_b} + \frac{\tan\frac{\theta_b}{2}\cos\theta_a}{Z_b}\right) & \cos\theta_a - \frac{Z_a \sin\theta_a \tan\frac{\theta_c}{2}}{Z_c} \end{bmatrix} \quad (1)$$

$$\begin{bmatrix} A_o & B_o \\ C_o & D_o \end{bmatrix} = \begin{bmatrix} \cos\theta_a + \frac{Z_a \sin\theta_a}{Z_b \tan(\theta_b/2)} & \mathrm{j}Z_a \sin\theta_a \\ \mathrm{j}\left(-\frac{\cos\theta_a}{\tan(\theta_c/2)Z_c} + \frac{\sin\theta_a}{Z_a} - \frac{Z_a \sin\theta_a}{Z_c Z_b \tan(\theta_c/2)\tan(\theta_b/2)} - \frac{\cos\theta_a}{\tan(\theta_b/2)Z_b}\right) & \cos\theta_a + \frac{Z_a \sin\theta_a}{Z_c \tan(\theta_c/2)} \end{bmatrix} \quad (2)$$

In the above, subscripts e and o denote the even- and odd-modes, respectively. The S-parameters of the power divider can be expressed through the normalized source inputs of the even- and odd-mode equivalent circuits as [1]:

$$\begin{cases} S_{11} = \frac{1}{2}\Gamma_e + \frac{1}{2}\Gamma_o = \frac{1}{2}\left(\frac{A_e Z_0 + B_e - C_e Z_0^2 - D_e Z_0}{A_e Z_0 + B_e + C_e Z_0^2 + D_e Z_0} + \frac{A_o Z_0 + B_o - C_o Z_0^2 - D_o Z_0}{A_o Z_0 + B_o + C_o Z_0^2 + D_o Z_0}\right) \\ S_{21} = \frac{1}{2}\Gamma_e - \frac{1}{2}\Gamma_o = \frac{1}{2}\left(\frac{A_e Z_0 + B_e - C_e Z_0^2 - D_e Z_0}{A_e Z_0 + B_e + C_e Z_0^2 + D_e Z_0} - \frac{A_o Z_0 + B_o - C_o Z_0^2 - D_o Z_0}{A_o Z_0 + B_o + C_o Z_0^2 + D_o Z_0}\right) \\ S_{31} = \frac{1}{2}T_e - \frac{1}{2}T_o = \frac{1}{2}\left(\frac{2Z_0}{A_e Z_0 + B_e + C_e Z_0^2 + D_e Z_0} - \frac{2Z_0}{A_o Z_0 + B_o + C_o Z_0^2 + D_o Z_0}\right) \\ S_{32} = \frac{1}{2}T_e + \frac{1}{2}T_o = \frac{1}{2}\left(\frac{2Z_0}{A_e Z_0 + B_e + C_e Z_0^2 + D_e Z_0} + \frac{2Z_0}{A_o Z_0 + B_o + C_o Z_0^2 + D_o Z_0}\right) \end{cases} \quad (3)$$

For rigorous design perspectives, including perfect matching ($S_{11} = 0$), ideal isolation ($S_{32} = 0$), predefined phase difference ψ ($\psi = \angle S_{21} - \angle S_{31}$) and power division ratio G ($G = |S_{21}|/|S_{31}|$) at the operation frequency f_0, the mathematical relationship of $ABCD$ parameters of equivalent subcircuits can be summarized as:

$$\begin{cases} A_e + B_e = -C_o - D_o \\ A_o + B_o = -C_e - D_e \\ \left|\frac{A_e - D_e + 2B_e}{2}\right| = G \\ \angle\frac{A_e - D_e + 2B_e}{2} = \psi \end{cases} \quad (4)$$

Substituting Eqs. (1) and (2) into Eq. (4) and after some algebraic manipulation, the final design formulas can be obtained as:

$$\begin{cases} Z_a = Z_0 \left|\sin\psi\right| G \\ Z_b = Z_c = Z_0 \left|\sin\psi\right| \sqrt{\frac{G^2}{1+G^2\sin^2\psi}} \\ \theta_a = \begin{cases} 90^\circ & \text{if } 0^\circ < \psi < 180^\circ \\ 270^\circ & \text{if } 180^\circ < \psi < 360^\circ \end{cases} \\ \theta_c = \begin{cases} a\cos\left[-\sqrt{\frac{G^2}{G^2+1}}\cos\psi\right] & \text{if } 0^\circ < \psi < 180^\circ \\ 180^\circ - a\cos\left[-\sqrt{\frac{G^2}{G^2+1}}\cos\psi\right] & \text{if } 180^\circ < \psi < 360^\circ \end{cases} \\ \theta_b = 180^\circ - \theta_c \end{cases} \tag{5}$$

It is obvious that this proposed power divider is unable to realize the phase difference $\psi = 0^\circ$ and 180° according to Equation (5). So this structure is defined as a quasi-arbitrary phase difference power divider. In the next section, the bandwidth performance, characteristic impedance and electrical length variations against power division ratio and phase difference will be further analyzed.

3. ANALYSES

Having formulated power divider design in the previous section, the characteristic impedances, electrical length and fractional bandwidth variations with the power division ratio and phase difference are analyzed here by using Matlab software. For the prototype built on a Rogers 4350B substrate of thickness 0.508 mm and dielectric constant 3.48, the maximum realizable characteristic impedance is about 150 Ω for a 3 mil line width. Because the port impedance Z_0 is typically 50 Ω, the normalized characteristic impedance is limited within the range from 0 to 3 to better clarify the feasible power and phase applications. In this section, the fractional bandwidth is defined as a frequency span meeting the following requirements simultaneously: acceptable matching and isolation ($|S_{11}| < -15$ dB and $|S_{32}| < -15$ dB), within 0.7 dB amplitude imbalance ($|S_{21}|/|GS_{31}| < \pm 0.7$ dB) and 5° phase imbalance (±5°) for port 2 and port 3.

3.1. The Variations with Power Division Ratio

The normalized characteristic impedance, electrical length of every transmission line and bandwidth variations with power division ratio are considered when three different phase difference outputs 60°,

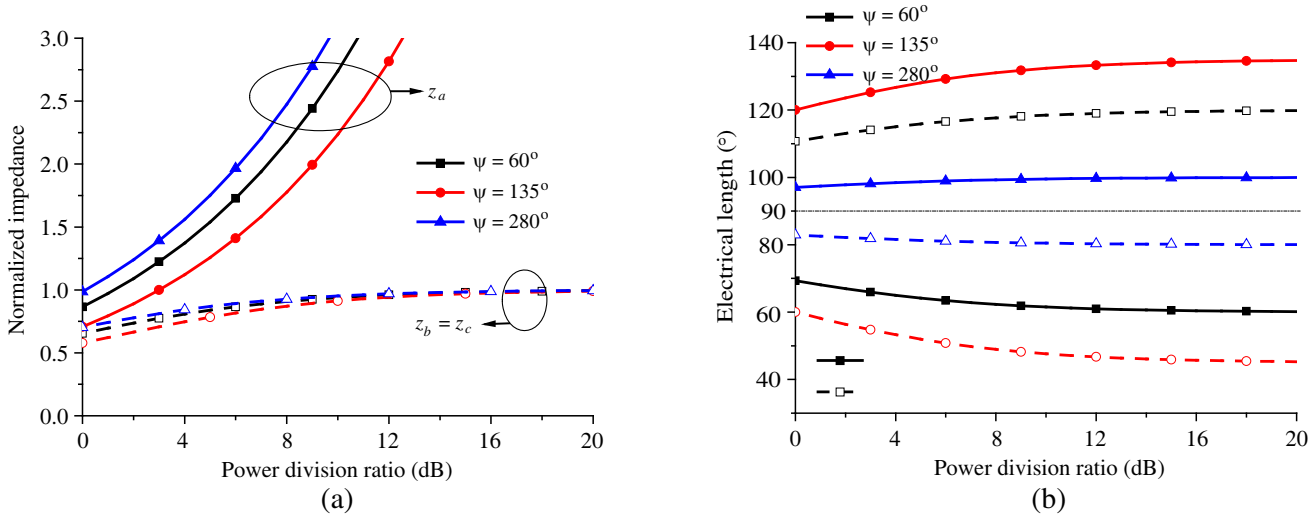

Figure 3. (a) The normalized characteristic impedance and (b) electrical length of every transmission line variations versus power division ratio for $\psi = 60^\circ$, 135°, 280°.

135°, 280° are chosen.

The normalized characteristic impedance and electrical length values varying with power division ratio are calculated and shown in Figure 3. From Figure 3(a), it can be seen that all characteristic impedances increase with the growth of power division ratio, and Z_a is always greater than Z_b and Z_c. The maximum value of Z_b (Z_c) is Z_0 when the power division ratio rises towards infinity, while the value of Z_a may be beyond the limit of attainable impedance. Therefore, the attainable power division ratio is determined by Z_a. On the other hand, the curves of electrical length become flat as power division ratio increases in Figure 3(b). Due to the relationship of $\theta_b = 180° - \theta_c$, the curves of θ_b are symmetric with θ_c with respect to electrical length 90°.

Figure 4 illustrates the fractional bandwidth as a function of power division ratio, which shows that in most cases the bandwidth increases when power division ratio increases.

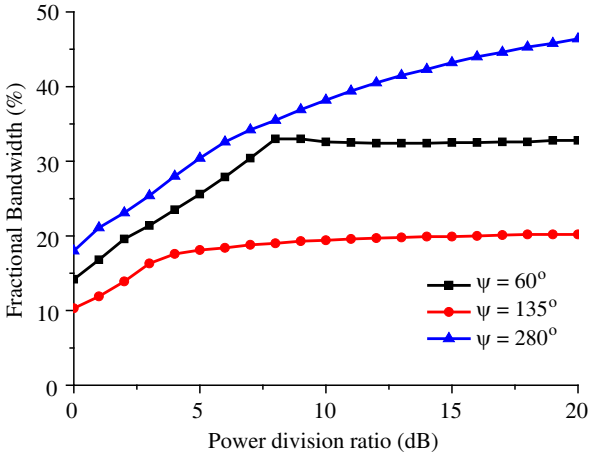

Figure 4. Bandwidth variations versus power division ratio for $\psi = 60°$, 135°, 280°.

3.2. The Variations with Phase Difference

In this section, the normalized characteristic impedance, electrical length of every transmission line and bandwidth variations are studied with respect to the phase difference for three power division ratios of

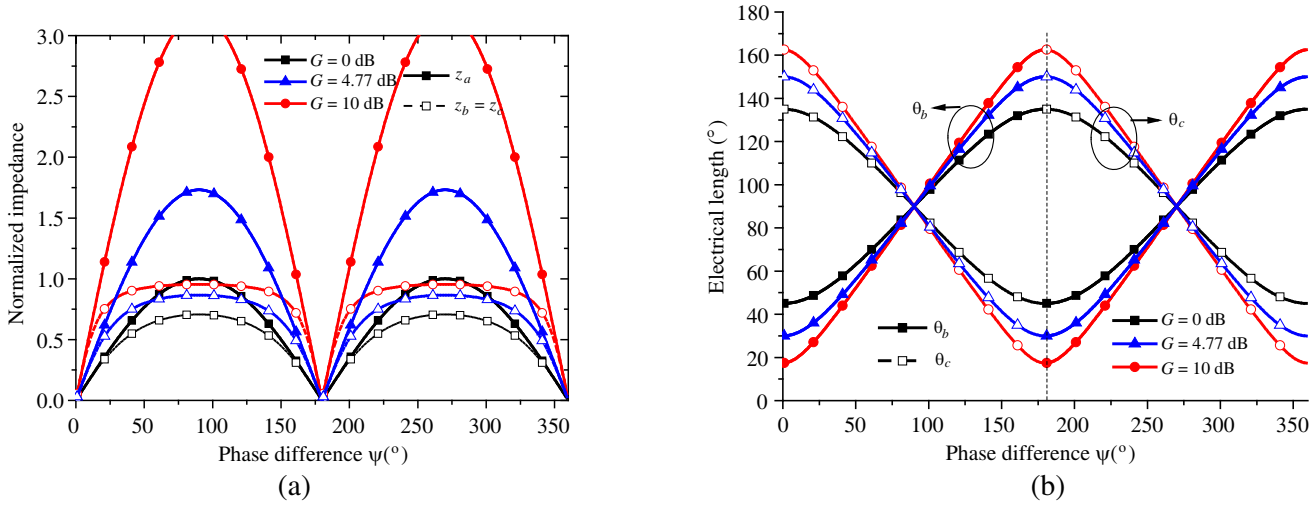

Figure 5. (a) The normalized characteristic impedance and (b) electrical length of every transmission line variations versus phase difference for $G = 0\,\text{dB}$, $4.77\,\text{dB}$, and $10\,\text{dB}$.

$G = 0\,\text{dB}$, 4.77 dB, and 10 dB.

The normalized characteristic impedance and electrical length values are calculated and plotted in Figure 5. As shown in Figure 5(a), the graph is symmetric against phase difference $\psi = 180°$. The maximum impedance values all occur at the point of phase difference $\psi = 90°$ or 270°. When power division G is 10 dB, the impedance of Z_a is partly beyond the limit of attainable impedance so that some phase differences cannot be realized, i.e., the available phase difference range will change with different power-dividing ratios. By calculation, when power division is below 9.54 dB, all the phase differences can be obtained except for 0° and 180°.

In Figure 5(b), the electrical length curves of θ_b and θ_c are both periodic with the period of $\psi = 180°$. During a single period, the curves of θ_b are monotonically increasing while the curves of θ_c are the opposite. The curves of θ_b are symmetric with θ_c not only against electrical length 90° but also against phase difference $\psi = 180°$. Furthermore, we can find that the higher the power division ratio is, the higher the swing amplitude of the curves is.

The bandwidth performance versus phase difference is shown in Figure 6. It is obvious that the period of the curves is $\psi = 180°$. The maximum bandwidth values for $G = 0\,\text{dB}$, 4.77 dB, 10 dB are 18.6%, 30.5%, 39.7%, respectively, located around phase difference $\psi = 90°$ or 270°.

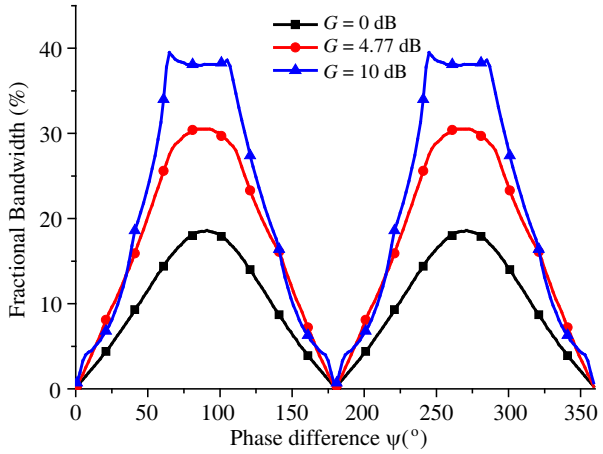

Figure 6. Bandwidth variations versus phase difference for $G = 0\,\text{dB}$, 4.77 dB, and 10 dB.

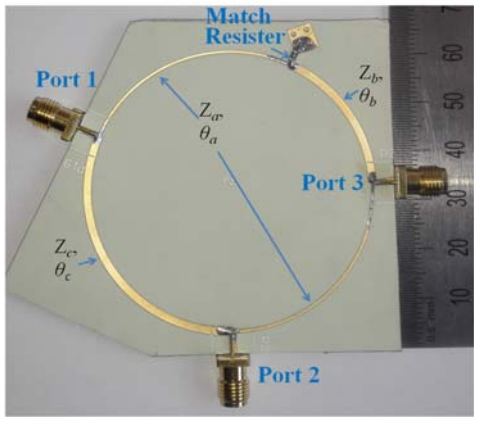

Figure 7. The photograph of the prototype.

4. EXPERIMENT

To consolidate the proposed concept experimentally, a prototype operating at 1 GHz is designed. The allocated power division G is 2 (6.02 dB), and phase difference ψ is 60°, which proves the capability for quasi-arbitrary phase difference and power division. According to the above method, the design parameters can be calculated and are listed in Table 1. The prototype has been fabricated on a 0.508 mm-thick Rogers 4350B substrate, with relative permittivity of $\varepsilon_r = 3.48$ and loss tangent of 0.003. A photograph of this prototype is shown in Figure 7.

Table 1. The design parameters of the prototype.

	Z_a	Z_b	Z_c	θ_a	θ_b	θ_c
Values	86.6 Ω	43.3 Ω	43.3 Ω	90°	63.4°	116.6°

Figure 8 shows the comparison between the simulated and measured magnitude and phase difference responses of the prototype using ADS software and Rohde & Schwarz ZVL vector network analyzer. It can be observed that the measured responses are in close agreement with the simulation. At the

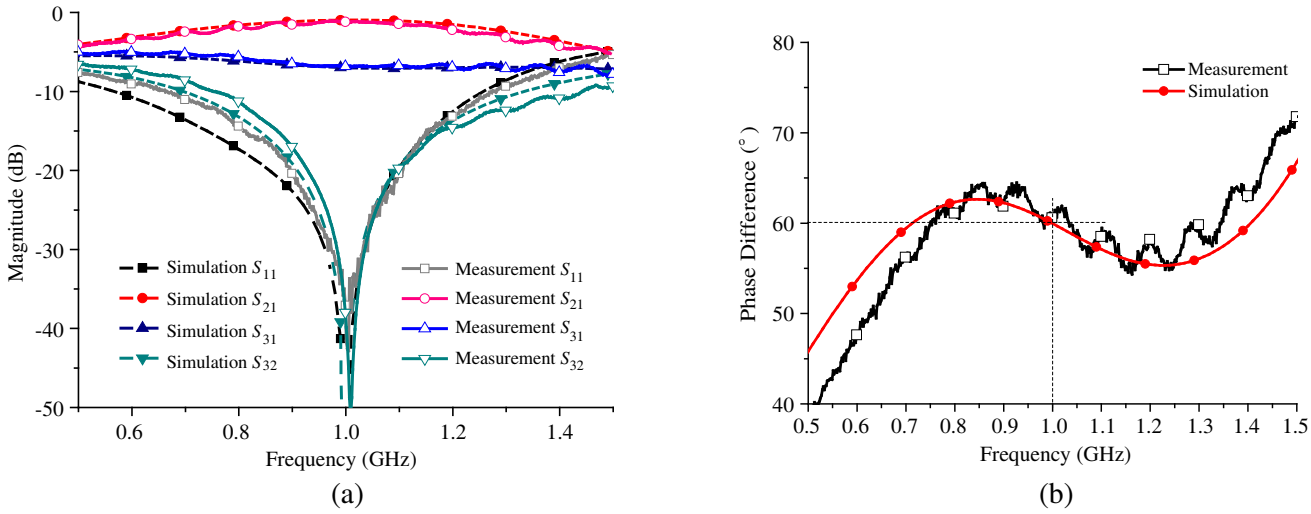

Figure 8. The S-parameters of the prototype: (a) the amplitude responses and (b) the phase difference responses.

operating frequency, the measured return losses and isolation parameters are both better than -30 dB. The power division ratio is 5.73 dB with the insertion loss of $|S_{21}| - 1.17$ dB and $|S_{31}| - 6.80$ dB, and the phase difference between port 2 and port 3 is 60.8°, which is close to the target. It demonstrates that the prototype fulfills the function of quasi-arbitrary phase difference with good power division performance at the operating frequency. The measured fractional bandwidth is 17.1% (from 0.930 GHz to 1.101 GHz) which is defined as $|S_{11}| < -20$ dB, $|S_{32}| < -20$ dB, $|S_{21}| = -1.17\,\text{dB} \pm 0.3$ dB, $|S_{31}| = -6.80\,\text{dB} \pm 0.5$ dB and $\angle S_{21} - \angle S_{31} = 60° \pm 5°$.

5. CONCLUSION

A novel unequal power divider for quasi-arbitrary phase difference has been proposed in this paper. It can be easily constructed using four microstrip lines and a matching resister. The explicit design formulas have been derived using even-odd mode analysis. Moreover, the normalized characteristic impedance, electrical length and bandwidth variations with power division ratio and phase difference are analyzed by simulation. As an experimental verification, a microstrip example with power division ratio 6.02 dB as well as 60° phase difference has been designed, implemented and measured. It works well as a conventional unequal power divider at the operating frequency, meanwhile excellently outputting assigned phase difference, which meets the requirement of quasi-arbitrary phase difference for actual application.

ACKNOWLEDGMENT

This work was supported in part by the program for Changjiang scholars and innovative research team in university (No. IRT1212), the project of construction of innovative teams and teacher career development for universities and colleges under Beijing Municipality (No. IDHT20130518).

REFERENCES

1. Pozar, D. M., *Microwave Engineering*, Wiley, New York, 2006.
2. Miao, C., X. Zheng, J. Yang, and W. Wu, "A symmetrical outputs uniplanar out-of-phase power divider without phase shifter," *Progress In Electromagnetics Research Letters*, Vol. 48, 95–101, 2014.

3. Chen, H., T. Zhang, W. Che, W. Feng, and Q. Xue, "Unequal Wilkinson power divider with wide range of arbitrary power division based on recombinant technology," *IET Microwaves, Antennas & Propagation*, Vol. 9, No. 2, 166–175, 2015.
4. Yin, K., "Millimeter wave power-combined amplifier using travelling-wave power divider-combiner," *2015 Asia-Pacific Microwave Conference (APMC)*, 1–3, Nanjing, China, 2015.
5. Choi, S. and J. Choi, "Dual-polarised antenna using unbalanced power dividers for small-cell base stations," *Electron. Lett.*, Vol. 52, No. 6, 419–421, 2016.
6. Mao, S.-G. and Y.-Z. Chueh, "Broadband composite right/left-handed coplanar waveguide power splitters with arbitrary phase responses and balun and antenna applications," *IEEE Transactions on Antennas and Propagation*, Vol. 54, No. 1, 243–250, 2006.
7. Deng, P.-H., J.-H. Guo, and W.-C. Kuo, "New Wilkinson power dividers based on compact stepped-impedance transmission lines and shunt open stubs," *Progress In Electromagnetics Research*, Vol. 123, 407–426, 2012.
8. Zhang, H., X.-W. Shi, F. Wei, and L. Xu, "Compact wideband Gysel power divider with arbitrary power division based on patch type structure," *Progress In Electromagnetics Research*, Vol. 119, 395–406, 2011.
9. Li, B., X. Wu, N. Yang, and W. Wu, "Dual-band equal/unequal Wilkinson power dividers based on coupled-line section with short-circuited stub," *Progress In Electromagnetics Research*, Vol. 111, 163–178, 2011.
10. Hayashi, H., H. Okazaki, A. Kanda, T. Hirota, and M. Muraguchi, "Millimeter-wave-band amplifier and mixer MMICs using a broad-band 45° power divider/combiner," *IEEE Transactions on Microwave Theory and Techniques*, Vol. 46, No. 6, 811–819, 1998.
11. Morimoto, K., J. Hirokawa, and M. Ando, "Design of a 180-degree single-layer divider to control sidelobe and crossover levels in butler-matrix beam-switching antenna," *2007 Asia-Pacific Microwave Conference (APMC 2007)*, 1–4, Bangkok, Thailand, 2007.
12. Kao, J. C., Y.-H. Hsiao, K.-S. Yeh, C.-C. Chiong, Y.-H. Lin, K.-Y. Lin, and H. Wang, "A 25-to-45-GHz 45° power divider," *2013 European Microwave Conference (EuMC)*, 959–962, Nuremberg, Germany, 2013.
13. Shi, J. and K. Xu, "Compact differential power divider with enhanced bandwidth and in-phase or out-of-phase output ports," *Electron. Lett.*, Vol. 50, No. 17, 1209–1211, 2014.
14. Song, K., Y. Mo, Q. Xue, and Y. Fan, "Wideband four-way out-of-phase slotline power dividers," *IEEE Transactions on Industrial Electronics*, Vol. 61, No. 7, 3598–3606, 2014.
15. Ahmed, U. T. and A. M. Abbosh, "Wideband out-of-phase power divider using tightly coupled lines and microstrip to slotline transitions," *Electron. Lett.*, Vol. 52, No. 2, 126–128, 2016.